Dalton Transactions

ROYAL SOCIETY OF CHEMISTRY

PAPER

View Article Online
View Journal | View Issue

Cite this: *Dalton Trans.*, 2023, **52**, 6426

Tetra-, tetradeca- and octadecametallic clusters of Mn†

Eleftheria Agapaki, Angelos B. Canaj, Gary S. Nichol and Euan K. Brechin *

Reaction of equimolar amounts of $MnBr_2{\cdot}4H_2O$ and HL^1 ((3,5-dimethyl-1*H*-pyrazol-1-yl)methanol) in a basic MeCN solution leads to the formation of $[Mn^{II}_4(L^1)_4Br_4(H_2O)_4]$ (**1**), whose metallic skeleton is a $[Mn^{II}_4]$ tetrahedron and cluster core a $[Mn^{II}_4(\mu_3\text{-}O)_4]$ cubane. Replacing $MnBr_2{\cdot}4H_2O$ with $Mn(O_2CMe)_2{\cdot}4H_2O$ affords $[Mn^{III}_2Mn^{II}_{12}O_2(L^1)_4(OAc)_{22}]$ (**2**) which is best described as a series of edge-sharing $[Mn_4]$ tetrahedra that have self-assembled into a linear array in which each $[Mn_2]$ pair is 'twisted' with respect to its neighbours in a corkscrew-like manner. Employment of the triangle $[Mn^{III}_3O(OAc)_6(py)_3](ClO_4)$ as a reactant instead of a Mn^{II} salt results in the formation of $[Mn^{III}_{14}Mn^{II}_4O_{14}(L^1)_4(HL^1)_2(OAc)_{18}(H_2O)_2]$ (**3**) whose core is comprised of three vertex-sharing $[Mn^{III}_4]$ butterflies flanked on either side by one $[Mn^{III}_4]$ cubane and one $[Mn^{III}_2Mn^{II}_2]$ tetrahedron. Dc magnetic susceptibility and magnetisation measurements of polycrystalline samples of **1–3** reveal the predominance of antiferromagnetic exchange interactions. For $[Mn_4]$ (**1**) this leads to a diamagnetic ground state, while for $[Mn_{18}]$ (**3**) competing exchange interactions result in Single-Molecule Magnet (SMM) behaviour with U_{eff} = 22 K.

Received 9th March 2023,
Accepted 18th April 2023

DOI: 10.1039/d3dt00732d

rsc.li/dalton

Introduction

The magnetic properties of molecules containing 3d transition metal ions have retained immense scientific interest for decades, originating from initial magneto-structural studies of metal dimers and trimers,[1] the construction of models for metalloenzymes[2] and the discovery of single-molecule and single-ion magnets,[3] to the investigation of geometric spin frustration,[4] the exploitation of enhanced magnetocaloric effects for cryogenic refrigeration[5] and the emergence of electron-spin based qubits for quantum computation.[6] The starting point for all such studies lies in the synthesis of new molecules, and the design of complexes with specific structural characteristics that promote targeted magnetic properties.[7] When polymetallic systems are sought-after the nature of the bridging ligands becomes paramount, and for larger nuclearity complexes 'small and simple' ligands are often particularly attractive since they offer flexibility in bonding due to (a) the number of coordination modes available, (b) the lack of steric constraints, (c) the ability to accommodate variable metal coordination numbers and geometries, and (d) the ability to stabilise multiple metal oxidation states.[8] Alongside the ubiquitous carboxylates,[9] N/O-chelate ligands have proved to be highly successful with pertinent examples including amino alcohols,[10] polyalkoxides[11] and oximes[12] (Scheme 1).

The pro-ligand (3,5-dimethyl-1*H*-pyrazol-1-yl)methanol (HL^1) belongs to the family of N/O-chelates and has previously been employed to make mono-, di- and tetrametallic compounds of Cu^{II}, Ni^{II} and Co^{II}.[13] In Fe chemistry there is just one example, an $[Fe_8]$ cage,[14] while there are four examples in Mn chemistry ranging in nuclearity between $[Mn_7]$ and $[Mn_{19}]$.[15] The relative sparsity of polymetallic cluster compounds reported suggests the ligand has been underemployed,

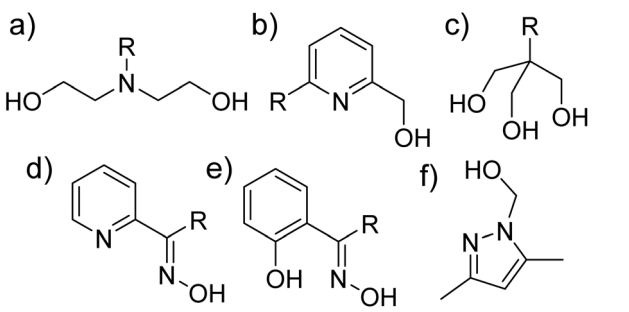

Scheme 1 Examples of organic pro-ligands successfully employed to synthesise polymetallic complexes of paramagnetic 3d metal ions. (a) Substituted diethanolamines (R-deaH$_2$, R = H, Me, Et, *etc.*; teaH$_3$, R = CH_2CH_2OH), (b) (2-hydroxymethyl)pyridines (R = H, hmpH; R = CH_2OH, pdmH$_2$), (c) tripodal alcohols (R = H, H$_3$thme; R = CH_2OH, H$_4$peol), (d) pyridyl oximes (R-paoH) and (e) phenolic oximes (R-saoH$_2$), (f) HL^1, employed here.

EaStCHEM School of Chemistry, The University of Edinburgh, David Brewster Road, Edinburgh, EH9 3FJ Scotland, UK. E-mail: ebrechin@ed.ac.uk

†Electronic supplementary information (ESI) available. CCDC 2233436 (**1**), 2233437 (**3**) and 2233438 (**2**). For ESI and crystallographic data in CIF or other electronic format see DOI: https://doi.org/10.1039/d3dt00732d

especially given the fascinating topologies already discovered. Here we expand its coordination chemistry to include the synthesis, structure and magnetic characterisation of three new Mn clusters – a $[Mn^{II}_4]$ cubane, a $[Mn^{III}_2Mn^{II}_{12}]$ cluster comprising a 'linear' array of six shared tetrahedra, and a $[Mn^{III}_{14}Mn^{II}_4]$ complex containing a $[Mn_{14}]$ plane of vertex- and edge-sharing $[Mn_4]$ butterflies, with the four capping ions forming $[Mn^{III}_4]$ cubanes and $[Mn^{III}_2Mn^{II}_2]$ tetrahedra with the core.

Experimental

All chemicals were purchased from commercial suppliers and used without further purification. HL^1 was prepared as previously described.[16] Elemental analyses were performed by the University of Edinburgh microanalytical service in the School of Geosciences.

Synthesis of $[Mn^{II}_4(L^1)_4Br_4(H_2O)_4]\cdot 2.25MeCN$ (1·2.25MeCN)

$MnBr_2\cdot 4H_2O$ (287 mg, 1 mmol), HL^1 (126 mg, 1 mmol) and NEt_3 (140 μL, 1 mmol) were dissolved in MeCN (15 mL) and stirred for 1 hour. The solution was then filtered and allowed to stand. Pale pink crystals of **1** grew upon slow evaporation of the mother liquor over 2 days. Elemental analysis (%) calculated for $Mn_4O_8N_8C_{24}H_{44}Br_4$: C, 25.92; H, 3.99; N, 10.08. Found: C, 26.00; H, 4.05; N, 10.07. Yield ≤ 40%.

Synthesis of $[Mn^{III}_2Mn^{II}_{12}O_2(L^1)_4(OAc)_{22}]\cdot 1MeCN\cdot 1C_3H_6O$ (2·1MeCN·1C$_3$H$_6$O)

$Mn(O_2CMe)_2\cdot 4H_2O$ (247 mg, 1 mmol), HL^1 (126 mg, 1 mmol) and NEt_3 (140 μL, 1 mmol) were dissolved in MeCN (15 mL) and stirred for 1 hour. The solution was then filtered and diffused with acetone. Brown crystals of **2** were obtained over 2 days. Elemental analysis (%) calculated for $Mn_{14}O_{55}N_8C_{68}H_{100}$: C, 30.49; H, 3.76; N, 4.18. Found: C, 30.75; H, 4.09; N, 4.04. Yield ≤ 30%.

Synthesis of $[Mn^{III}_{14}Mn^{II}_4O_{14}(L^1)_4(HL^1)_2(OAc)_{18}(H_2O)_2]\cdot 2.5MeCN$ (3·2.5MeCN)

$[Mn_3O(OAc)_6(py)_3](ClO_4)$ (871 mg, 1 mmol), HL^1 (252 mg, 2 mmol) and NEt_3 (280 μL, 2 mmol) were dissolved in MeCN (15 mL) and stirred for 1 hour. The solution was then filtered and diffused with Et_2O. Dark brown crystals of **3** were obtained over 2 days. Elemental analysis (%) calculated for $Mn_{18}O_{61}N_{12}C_{72}H_{120}$: C, 27.73; H, 3.88; N, 5.39. Found: C, 27.44; H, 3.76; N, 5.39. Yield ≤ 45%.

Single crystal X-ray diffraction data for 1–3

Suitable crystals of **1–3** were selected and mounted on a MITIGEN holder in Paratone oil on either a Rigaku Oxford Diffraction XCalibur (**1**) or SuperNova (**2**, **3**) diffractometer. Crystals were kept at T = 120 K (**1**, **2**) or 100 K (**3**) during data collection. The structures were solved with the ShelXT program using dual methods with Olex2 as the graphical interface. Models were refined with ShelXL using full matrix least squares minimisation on F^2.[17]

Crystal data for 1. $C_{28.5}H_{50.75}Br_4Mn_4N_{10.25}O_8$, M_r = 1204.44, triclinic, $P\bar{1}$ (no. 2), a = 10.1989(2) Å, b = 12.8405(3) Å, c = 18.4168(3) Å, α = 99.820(2)°, β = 90.437(2)°, γ = 105.874(2)°, V = 2282.13(8) Å^3, T = 120.00(11) K, Z = 2, Z' = 1, μ(MoK$_\alpha$) = 4.636, 87 672 reflections measured, 15 804 unique (R_{int} = 0.0479) which were used in all calculations. The final wR_2 was 0.0626 (all data) and R_1 was 0.0332 ($I \geq 2\sigma(I)$). CCDC 2233436.†

Crystal data for 2. $C_{73}H_{111}Mn_{14}N_9O_{51}$, M_r = 2699.86, orthorhombic, *Fddd* (no. 70), a = 15.1080(2) Å, b = 20.4454(4) Å, c = 76.1586(11) Å, $\alpha = \beta = \gamma$ = 90°, V = 23 524.6(7) Å^3, T = 120.01(10) K, Z = 8, Z' = 0.25, μ(MoK$_\alpha$) = 1.531, 49 597 reflections measured, 6437 unique (R_{int} = 0.0419) which were used in all calculations. The final wR_2 was 0.0799 (all data) and R_1 was 0.0329 ($I \geq 2\sigma(I)$). CCDC 2233438.†

Crystal data for 3. $C_{81}H_{121.5}Mn_{18}N_{16.5}O_{58}$, M_r = 3243.36, triclinic, $P\bar{1}$ (no. 2), a = 15.1254(4) Å, b = 15.3885(4) Å, c = 15.9092(3) Å, α = 103.925(2)°, β = 99.153(2)°, γ = 117.635(2)°, V = 3022.24(14) Å^3, T = 100.00(10) K, Z = 1, Z' = 0.5, μ(CuK$_\alpha$) = 15.573, 128 161 reflections measured, 11 063 unique (R_{int} = 0.1085) which were used in all calculations. The final wR_2 was 0.1365 (all data) and R_1 was 0.0486 ($I \geq 2\sigma(I)$). CCDC 2233437.†

Powder X-ray diffraction data for 1–3

Powder XRD data (Fig. S1–S3†) were collected on freshly prepared polycrystalline powder samples of **1–3** using a Bruker D8 ADVANCE with copper radiation at 40 kV, 40 mA and a Johansson monochromator, 2 mm divergence slit and 2.5 degree Soller slits on the incident beam side. LynxEye detector, Bruker DIFFRAC software. Diffraction measured from 2θ = 5°–40°, step size 0.0101°, using borosilicate capillaries of 0.7 mm outside diameter.

Magnetometry

Magnetic data for **1–3** were collected on freshly prepared polycrystalline samples restrained in eicosane in gelatine capsules on a Quantum Design PPMS Dynacool in the temperature range T = 300–2 K and field range B = 0.1–9.0 T. Diamagnetic corrections were applied using Pascal's constants.

Results and discussion

Reaction of equimolar amounts of $MnBr_2\cdot 4H_2O$ and HL^1 in a basic MeCN solution leads to the formation of pink crystals of $[Mn^{II}_4(L^1)_4Br_4(H_2O)_4]\cdot 2.25MeCN$ (**1**·2.25MeCN). Crystals were in a triclinic cell and structure solution was performed in the $P\bar{1}$ space group. The asymmetric unit contains the whole formula. The metallic skeleton of **1** (Fig. 1) describes a $[Mn^{II}_4]$ tetrahedron and the cluster core a $[Mn^{II}_4(\mu_3\text{-}O)_4]$ cube (Mn–O–Mn, ~98–102°; see Table S1† for BVS calculations). The μ_3-O-atoms are provided by the L^1 ligands, which chelate each metal centre and further bridge to two neighbouring metal ions. The Mn ions are all six-coordinate and in distorted octahedral geometries with their {MnO$_4$NBr} coordination spheres (Mn–O, ~2.2 Å; Mn–N, ~2.2 Å, Mn–Br, ~2.6 Å) completed by the presence of one Br anion and one H_2O molecule. The latter form

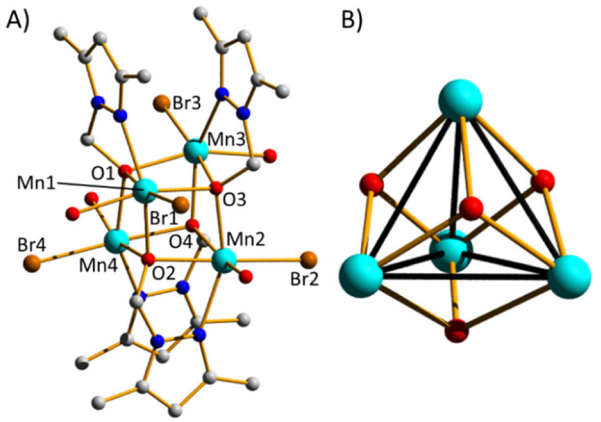

Fig. 1 (A) Molecular structure of complex **1** and (B) its metal–oxygen core. Colour code: Mn^{II} = light blue, C = grey, O = red, N = dark blue, Br = brown. H atoms and solvent of crystallisation omitted for clarity. The solid black lines in (B) highlight the tetrahedral arrangement of metal ions.

intramolecular H-bonds across four of the six faces of the cube (Br···(H)O, ~3.3 Å). They are also responsible for mediating intermolecular interactions between neighbouring clusters (Br···(H)O, ~3.3 Å) and to the MeCN molecules of crystallisation (O(H)···N, ~2.8 Å). The result is an intricate network of H-bonded clusters in the extended structure (Fig. S4†). A search of the Cambridge Structural Database (CSD) for $[Mn_4O_4]$ cubanes generates 87 hits, approximately 30% (26) of which are $[Mn^{II}_4O_4]$.

Repeating the reaction that produces **1** but replacing $MnBr_2{\cdot}4H_2O$ with $Mn(O_2CMe)_2{\cdot}4H_2O$ affords brown crystals of $[Mn^{III}_2Mn^{II}_{12}O_2(L^1)_4(OAc)_{22}]{\cdot}1MeCN{\cdot}1C_3H_6O$ (**2**·1MeCN·1C_3H_6O) when acetone is diffused into the MeCN mother liquor (Fig. 2A–C). Crystals were in an orthorhombic cell and structure solution was performed in the *Fddd* space group. The asymmetric unit contains one quarter of the formula. The metallic skeleton of **2** (Fig. 3A–C) describes a series of edge-sharing $[Mn_4]$ tetrahedra that have self-assembled into a linear array in which each $[Mn_2]$ pair is 'twisted' with respect to its neighbours in a corkscrew-like manner. In the centre of the cluster lies a $[Mn^{III}_2Mn^{II}_4(\mu_4\text{-}O)_2]$ unit (Fig. 2C) that consists of two edge-sharing $[Mn^{III}_2Mn^{II}_2]$ tetrahedra – the $\{Mn^{III}_2\}$ unit being the shared edge.

The μ_4-O^{2-} ion (O13 and symmetry equivalent, s.e.) links the two central Mn^{III} ions (Mn4 and s.e.) to each other and to two Mn^{II} ions on each side (Mn3 and s.e.). This $[Mn_6]$ unit is well documented in Mn carboxylate chemistry.[18] The $[Mn_6]$ unit is then connected on each side to a $[Mn^{II}_4]$ tetrahedron (Mn1, Mn2 and s.e.). The metals in the $[Mn_{14}]$ moiety are connected by a series of (twenty two) μ-, μ_3- and μ_4-carboxylates, while the μ_3-L^1 ligands are found at the periphery of the molecule, chelating to Mn1 (and s.e.) and further bridging to Mn2 (and s.e., Fig. S5†). All the metal ions are six-coordinate and in distorted octahedral geometries, with the two Mn^{III} ions displaying the expected Jahn–Teller (JT) elongation along the

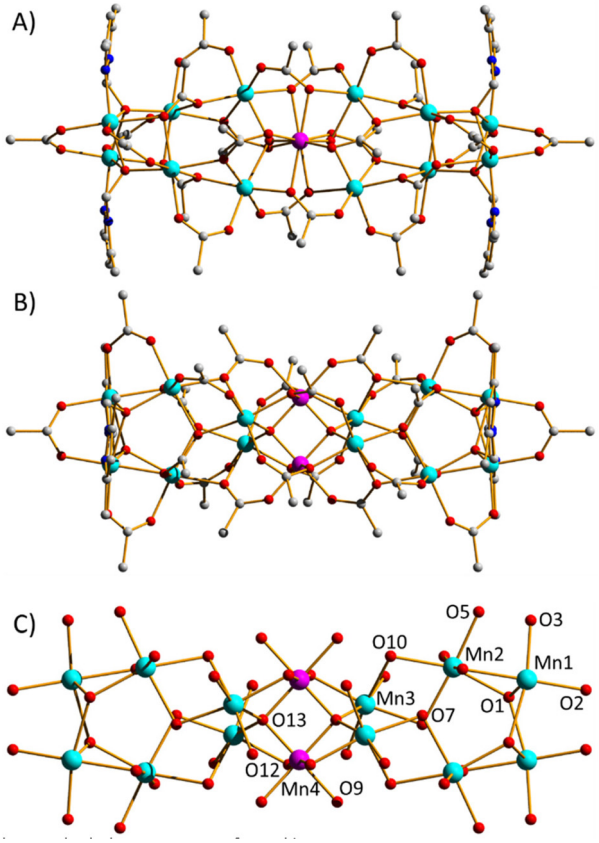

Fig. 2 Orthogonal views of the molecular structure of complex **2** viewed down the (A) *b*-axis, and (B) *a*-axis. (C) The metal–oxygen core of **2**. Colour code: Mn^{III} = pink, Mn^{II} = light blue, C = grey, O = red, N = dark blue. H atoms and solvent molecules of crystallisation omitted for clarity.

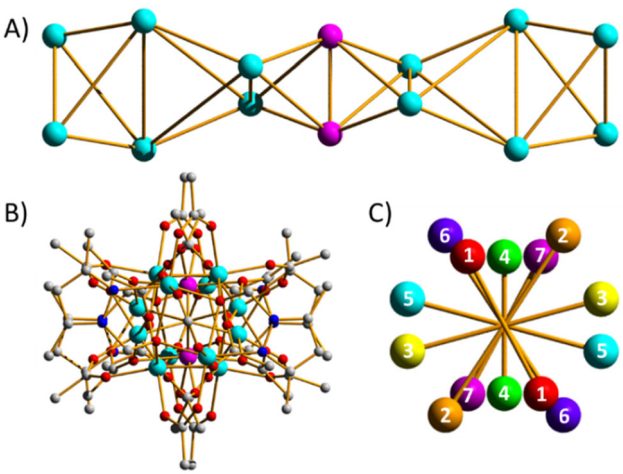

Fig. 3 (A) Metallic skeleton of **2** viewed down the *a*-axis. (B) Molecular structure of **2** viewed down the *c*-axis. (C) Colour/number coded sketch of the $\{Mn_2\}$ units in the same plane as viewed down the *c*-axis, highlighting the corkscrew arrangement (1 (red) → 2 (orange) → 3 (yellow) → 4 (green) → 5 (light blue) → 6 (dark blue) → 7 (purple)) of metal ions along the body of the cluster.

O12–Mn4–O12′ (and s.e.) vector. By symmetry, these are co-planar (Fig. S6†). Closest intermolecular interactions are observed between L^1 ligands (C(H)···(H)C, ~3.2–3.8 Å) and carboxylates (C(H)···O(C), ~3.2–3.6 Å), which results in the formation of a brickwork-like motif in the extended structure (Fig. S6†). There are sixteen [Mn_{14}] clusters deposited in the CSD, none with the topology or oxidation state distribution displayed by compound **2**.[19]

The reaction of $[Mn_3O(OAc)_6(py)_3](ClO_4)$ with HL^1 in a basic MeCN solution affords black crystals of $[Mn^{III}_{14}Mn^{II}_4O_{14}(L^1)_4(HL^1)_2(OAc)_{18}(H_2O)_2]\cdot 2.5MeCN$ (**3**·2.5MeCN) when Et_2O is diffused into the mother liquor (Fig. 4). The crystals were in a triclinic cell and structure solution was performed in the space group $P\bar{1}$. The asymmetric unit contains half the formula. The metallic skeleton of **3** has a $[Mn^{III}_{14}Mn^{II}_4]$ oxidation state distribution, the central part of which is a near-planar $[Mn^{III}_{10}Mn^{II}_2]$ disc (Mn1, Mn3–6, Mn8–9 and s.e.; where Mn5 is the +2 ion) which is constructed from seven vertex- and edge-sharing [Mn_4] butterflies (Fig. 5). Two Mn^{II} ions (Mn7 and s.e.) and two Mn^{III} ions (Mn2 and s.e.) lie 'above' and 'below' this plane forming distorted $[Mn^{III}_2Mn^{II}_2]$ and $[Mn^{III}_4]$ tetrahedra with three Mn ions in the planar disc, respectively. The metal–oxygen core describes three central vertex-sharing $[Mn^{III}_4O_2]$ butterflies (Mn8, Mn9, O11, O8, O9 and s.e.), flanked on either side by one $[Mn^{III}_4O_4]$ cubane (Mn1–4, O4, O5, O7, O14 and s.e.) and one $[Mn^{III}_2Mn^{II}_2O]$ tetrahedron (Mn1, Mn5–7, O6 and s.e.) (Fig. 5).

The acetate ligands are of three types (Fig. S7†). Fourteen are μ-bridging, two are μ_3-bridging (between Mn1, Mn2, Mn6 and s.e.) and two are μ_4-bridging (Mn1, Mn3, Mn4, Mn7 and s.e.) with the μ_3-O atom forming a corner of the $[Mn^{III}_4O_4]$ cubane. The four μ-L^{-1} ligands are found at the periphery of the cluster, chelating to Mn4 and Mn5 (and s.e.) and bridging to Mn5 and Mn6 (and s.e.), respectively. The two HL^1 ligands are found in the centre of the cluster, chelating to Mn7 (and s.e.) and forming a longer contact to Mn8 (and s.e.,

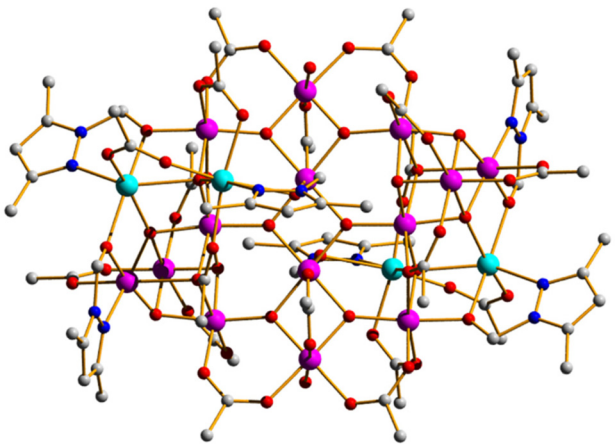

Fig. 4 Molecular structure of compound **3**. Colour code: Mn^{III} = pink, Mn^{II} = light blue, C = grey, O = red, N = dark blue. H atoms and solvent molecules of crystallisation omitted for clarity.

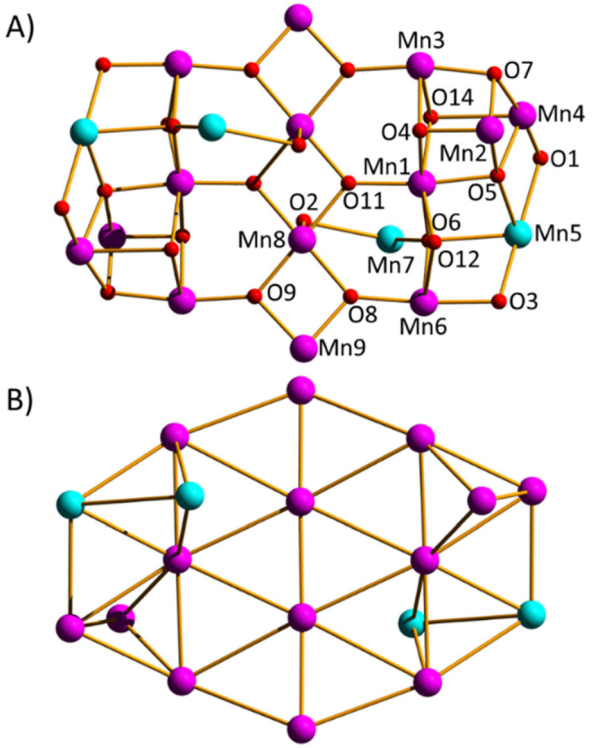

Fig. 5 (A) Metal–oxygen core of **3** minus the carboxylate O-atoms. (B) Metallic skeleton of **3**. Colour code: Mn^{III} = pink, Mn^{II} = light blue, O = red.

O–Mn, ~2.55 Å). The protonated O-atom is H-bonding to both a μ_3-O^{2-} ion (O···O, ~2.81 Å) and the O-atom of a bridging OAc (O···O, ~2.61 Å). The two H_2O molecules are bonded to Mn9 (and s.e.), H-bonding to the O-atoms of neighbouring μ-OAc ligands (~2.74–2.88 Å).

All the Mn ions in **3** are six-coordinate and in distorted octahedral geometries, with the Mn^{III} ions displaying their expected JT elongation (most of which are approximately co-parallel; Fig. S8†). The only exception is Mn8 (and s.e.) which is five coordinate and square pyramidal, the sixth coordination site being 'occupied' by the distal O2 atom of the protonated HL^1 ligand.

There are numerous inter-molecular interactions in the structure of **3**. The MeCN molecules of crystallisation are in close contact with bridging OAc ligands, C(H)···O, ~3.2 Å, as are peripheral L^1 and OAc ligands on neighbouring complexes (C/N/O···C/N/O, >3.3 Å). The result is that clusters of **3** pack in a brickwork-like fashion in the extended structure (Fig. S8†). A search of the CSD reveals ten [Mn_{18}] clusters. These include, two $[Mn^{III}_{15}Mn^{II}_3]$ super-tetrahedra built with triethanolamine,[20] a $[Mn^{III}_{18}]$ wheel of triangles using salicylaldoxime,[21] a $[Mn^{II}_8Mn^{III}_6Mn^{IV}_4]$ wheel of defective cubanes made from tripodal alcohols,[22] a $[Mn^{IV}_2Mn^{III}_{16}]$ cage stabilised with phosphonates,[23] dimers of $[Mn^{III}_9]$ molecules linked with 4,4′-bpy or diamagnetic metal ions,[24] a $[Mn^{III}_{14}Mn^{II}_4]$ carboxylate cage with the 'rock-salt' structure,[25] a $[Mn^{III}_{18}]$ super-octahedron built from a polydentate amino alcohol[26] and a near-planar $[Mn^{III}_{18}]$ cage constructed

from [Mn_4] butterflies and dicarboxylates.[27] While the latter has some structural similarity to **3**, the closest structural analogue is the complex $[Mn^{III}_{16}Mn^{II}_2O_{14}(O_2CMe)_{18}(hep)_4(hepH)_2(H_2O)_2](ClO_4)_2$, built with a different, but related N/O-chelate ligand (hepH = 2-(hydroxyethyl)pyridine).[28] This species has a similar Mn–O core and metallic skeleton, but a different oxidation state distribution.

Magnetic properties

Dc magnetic susceptibility (χ) and magnetisation (M) measurements of polycrystalline samples of **1–3** were collected in the T = 300–2 K, B = 0.1 T and T = 2–10 K, B = 0.5–9.0 T temperature and field ranges, respectively. These data are plotted in Fig. 6, 7 and S9.†

For **1** the χT value of 17.5 cm^3 K mol^{-1} at T = 300 K is as expected for four uncorrelated S = 5/2 spins, assuming g = 2.00 (Fig. 6). As T is decreased the value of χT remains essentially invariant until approximately T = 25 K wherefrom the value decreases to a minimum value of 4.4 cm^3 K mol^{-1} at T = 2 K. Magnetisation data (Fig. 7A) rise rapidly with increasing field saturating at a maximum value of 19.55 μ_B at T = 2 K and B = 9.0 T. Both are indicative of very weak, predominantly antiferromagnetic exchange interactions between the Mn^{II} ions (the large magnetisation value at B = 9 T is field induced).

The experimental susceptibility and magnetisation data for **1** can be simultaneously fitted with an isotropic spin-Hamiltonian $\hat{H} = -2\sum_{i<j} J_{ij}\hat{\vec{s}}_i \cdot \hat{\vec{s}}_j$ with a coupling scheme that assumes two unique exchange interactions between neighbouring Mn^{II} ions based on differing Mn–O–Mn angles (Fig. 8), J_1 = −0.19 cm^{-1} (between Mn1–Mn2, Mn1–Mn4, Mn2–Mn3 and Mn3–Mn4 with Mn–O–Mn ≥ 100.3°) and J_2 = +0.038 cm^{-1} (between Mn1–Mn3, Mn2–Mn4 with Mn–O–Mn ≤ 98.4°) with g = 2.0. The fit can be improved slightly by including a ferromagnetic intermolecular interaction, zJ = +6.72 × 10^{-3} cm^{-1}, consistent with the packing of the molecules and H-bonding in the extended structure. The intramolecular

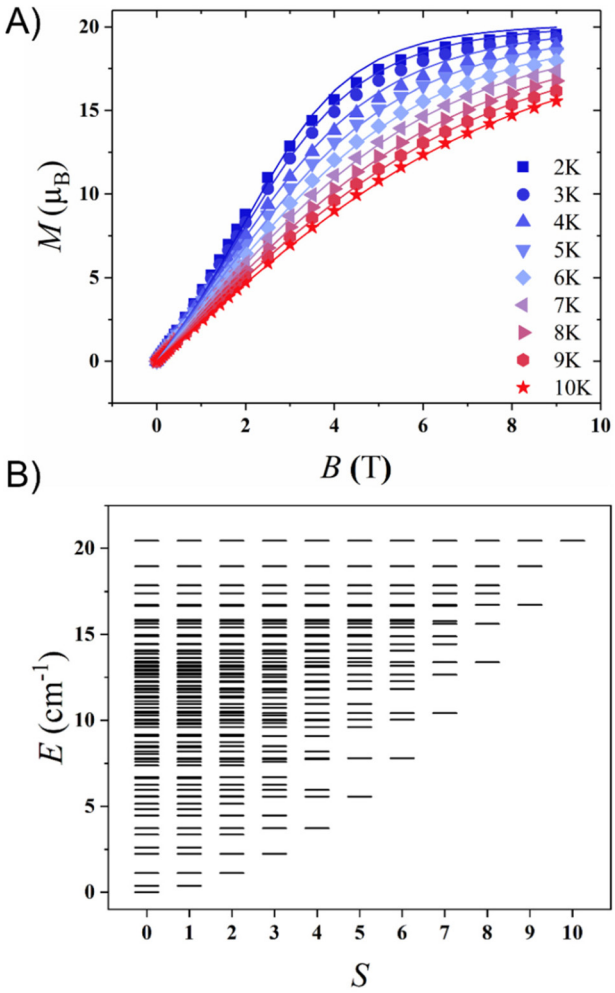

Fig. 7 (A) Magnetisation data for **1** collected in the T = 2–10 K and B = 0.5–9.0 T ranges, respectively. The solid lines are a best fit of the experimental data. See the main text for details. (B) Energy *vs.* spin state diagram for **1** derived from the simultaneous fit of the susceptibility and magnetisation data. The ground state is an S = 0 state, with multiple low-lying S states.

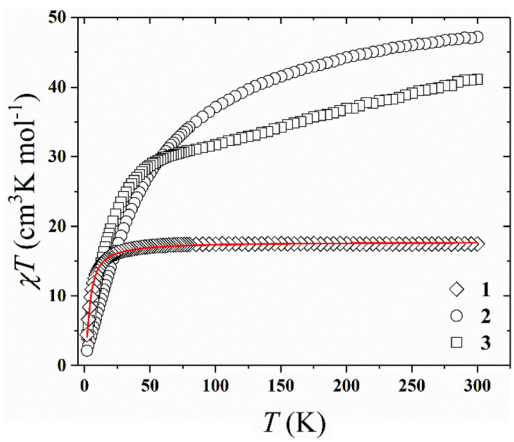

Fig. 6 Temperature dependence of magnetic susceptibility data plotted as the χT product *vs.* T for **1–3** under an applied field, B = 0.1 T. The solid red line represents the best fit of the experimental data for **1**. See text for details.

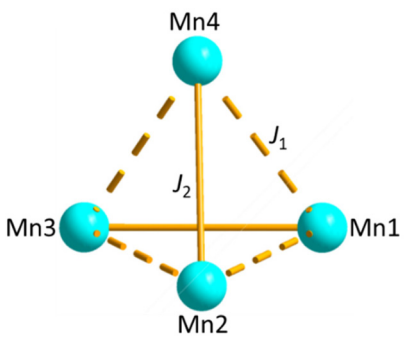

Fig. 8 Magnetic coupling scheme used to fit the magnetic susceptibility and magnetisation data for complex **1**. The different Mn–O–Mn angles present dictate that two different exchange interactions, J_1 and J_2, are employed. See text for details.

exchange coupling constants are consistent with values previously reported for alkoxide-bridged Mn^{II} cubes with similar Mn–O–Mn angles where the switch from ferro- to antiferromagnetic occurs at ~100°.[29] This leads to a ground state of S = 0 with multiple low-lying excited states (Fig. 7B).

Given that the magnitude of the exchange calculated is potentially of the same order of magnitude as that of the zero-field splitting expected for Mn^{II} ions in a distorted octahedral $\{MnO_4NBr\}$ coordination sphere[30] we have also fitted the susceptibility and magnetisation data by including single ion anisotropy $\left(\hat{H} = D\sum_j (\hat{s}_j)^2\right)$. The best fit afforded J_1 = −0.18 cm^{-1}, J_2 = +0.053 cm^{-1} and $|D|$ = 0.05 cm^{-1}, with g = 2.01 and zJ = +7.22 × 10^{-3} cm^{-1} (Fig. S9†). The fit is of slightly lower quality, but clearly reveals that J and D are correlated and thus while we can conclude a magnetic interaction of <|0.2| cm^{-1} is present, the exact contributions to that interaction are somewhat open to debate.

The χT value for **2** at T = 300 K (47.2 cm^3 K mol^{-1}) is below that expected for a $[Mn^{III}_2Mn^{II}_{12}]$ unit (58.5 cm^3 K mol^{-1}), assuming g = 2.00. The value of χT continuously decreases with decreasing temperature to a minimum value of 2.1 cm^3 K mol^{-1} at T = 2 K. Magnetisation data rise in a near linear fashion with increasing field and without saturating, reaching a maximum value of 13.92 μ_B at T = 2.0 and B = 9.0 T (Fig. S10†). Both are indicative of relatively weak antiferromagnetic exchange interactions between the Mn ions, likely resulting in a diamagnetic ground state but with multiple low-lying, paramagnetic excited states. Weak exchange is commonly observed in clusters with multiple Mn^{II} ions.[31] The nuclearity and complex topology of compound **2** preclude a quantitative analysis of the susceptibility and magnetisation data. A fit of the inverse susceptibility data ($1/\chi$ *vs.* T, Fig. S11A†) affords C = 54.9 cm^3 K mol^{-1} and θ = −48.6 K.

The χT value for **3** at T = 300 K (41.1 cm^3 K mol^{-1}) is below that expected for a $[Mn^{III}_{14}Mn^{II}_4]$ (59.5 cm^3 K mol^{-1}) unit, assuming g = 2.00. As T is decreased χT decreases steadily to a value of ~32 cm^3 K mol^{-1} at T = 100 K, before decreasing more slowly to a value of ~29 cm^3 K mol^{-1} at T = 50 K. Below this temperature χT decreases much more rapidly, to a minimum value of 4.4 cm^3 K mol^{-1} at T = 2 K. Magnetisation data for **3**

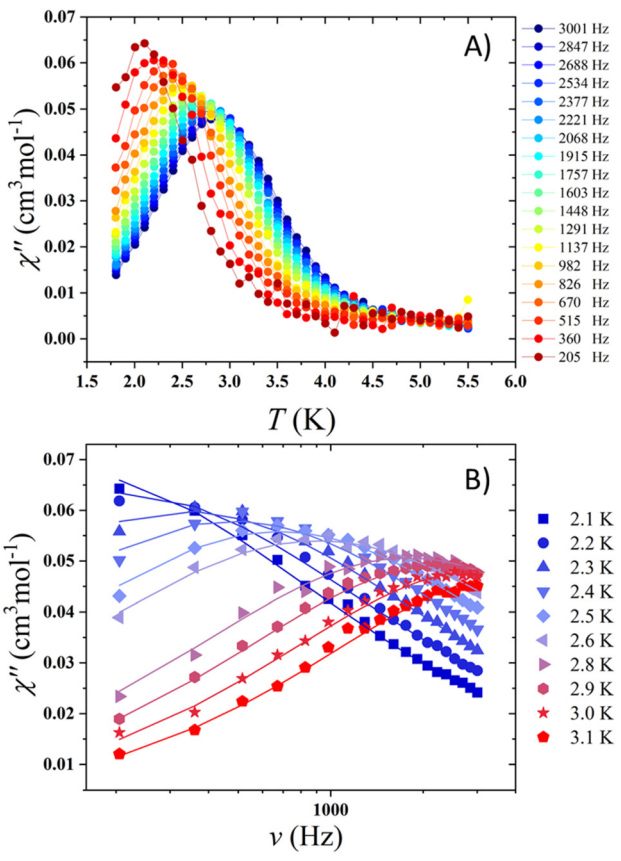

Fig. 9 (A) Temperature dependence of the out-of-phase, χ'', ac susceptibility in zero dc field for **3** with ac frequencies of 205–3001 Hz in the temperature range 1.8–6.0 K. (B) Frequency dependence of the out-of-phase, χ'', ac susceptibility for **3** up to 3.1 K in zero dc field. The solid lines correspond to the best fit to the Debye law.

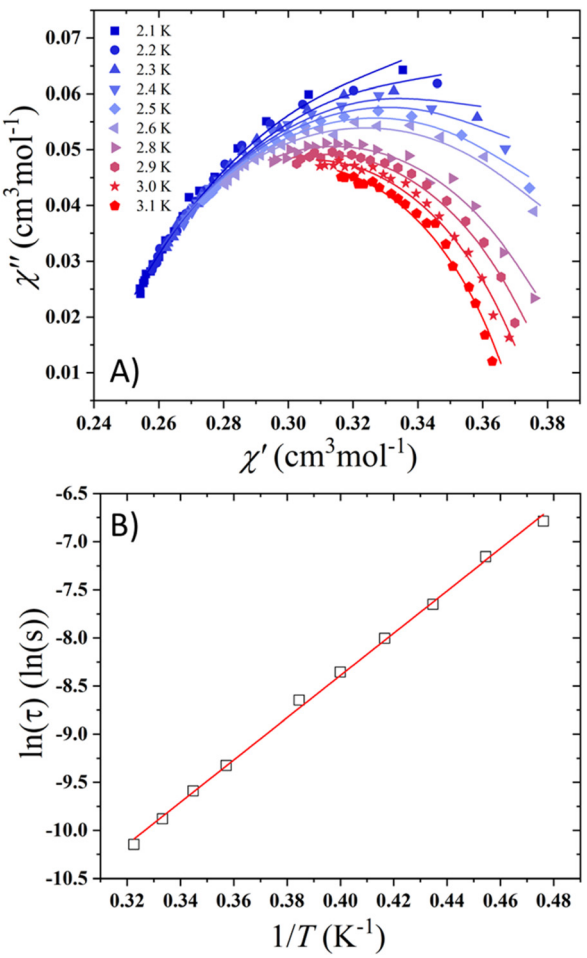

Fig. 10 (A) χ'' *vs.* χ' plot of the ac magnetic susceptibility data for **3** in zero dc field. The solid lines correspond to the best fit to the Debye law. (B) Plot of the relaxation time τ (logarithmic scale) *versus* T^{-1}. The solid red line represents the best fit to the Arrhenius law, yielding U_{eff} = 22 K.

initially rise in a near linear fashion with increasing field (B = 0.5–4.0 T), but thereafter rise more slowly and appear to begin to saturate at ~16.2 μ_B at T = 2.0 and B = 9.0 T (Fig. S10†). The data are therefore indicative of weak, but competing antiferromagnetic exchange interactions. A fit of the Curie–Weiss law (Fig. S11B†) affords C = 47.1 cm^3 K mol^{-1} and θ = −51.5 K.

Variable-temperature alternating current (ac) susceptibility measurements were performed to investigate the magnetic relaxation dynamics of **1–3**, with only **3** exhibiting frequency dependent out-of-phase χ'' ac susceptibility peaks at temperatures up to ~3.5 K in the absence of an external magnetic field (Fig. 9, 10 and S12–S15†). Relaxation times, τ, were extracted by fitting the Cole–Cole χ'' *vs.* χ' plots using the generalised Debye model. The data were analysed with CCFIT.[32] The distribution of the α parameter was found to be in the range 0.22 to 0.36 (2.1–3.1 K). An Arrhenius plot of the ln(τ) data *versus* the inverse temperature (T^{-1}) was fit to an Orbach process yielding U_{eff} = 22 K (15.3 cm^{-1}) and $\tau_0 = 3.5 \times 10^{-8}$ s. These values are consistent with other Mn-based single-molecule magnets assuming an Orbach-only relaxation process.[28]

Conclusions

The reaction of HL^1 with the Mn salts $MnBr_2{\cdot}4H_2O$ and $Mn(O_2CMe)_2{\cdot}4H_2O$ in basic MeCN solutions leads to the formation of $[Mn^{II}_4]$ and $[Mn^{III}_2Mn^{II}_{12}]$ clusters, respectively. The structure of the former is a cube and that of the latter best described as a series of tetrahedra that have self-assembled into a "twisted" linear array. Switching to the basic carboxylate $[Mn^{III}_3O(OAc)_6(py)_3](ClO_4)$ as a reactant results in the formation of a $[Mn^{III}_{14}Mn^{II}_4]$ cluster whose structure contains vertex-sharing $[Mn^{III}_4]$ butterflies flanked on either side by $[Mn^{III}_4]$ cubanes and $[Mn^{III}_2Mn^{II}_2]$ tetrahedra. In **1** and **2** the L^1 ligand acts solely as a μ_3-bridge helping to form an $[Mn^{II}_4O_4]$ cubane in each case, while in **3** it acts as a μ-bridge or remains protonated (HL^1) and acts as a simple chelate. Interestingly, the oxidation state distributions in **1** (Mn^{II}_4) and **2** ($Mn^{III}_2Mn^{II}_{12}$) are dominated by Mn^{II}, suggesting HL^1 to be less acidic than similar ligands such as hmpH, hepH and $pdmH_2$ (Scheme 1) which normally result in Mn^{III}-dominated clusters.[28,33] This is also reflected in the L^1 ligands always coordinating to at least one Mn^{II} ion in **1–3**. A larger ratio of Mn^{III} : Mn^{II} ($Mn^{III}_{14}Mn^{II}_4$, **3**) in the product can be obtained by employing an $[Mn^{III}_3]$ triangle as the reactant, although we note that there has been some metal reduction, hinting at some complex redox behaviour in the formation of **3**. For both **2** and **3** the ratio of OAc : L^1 in the complex is heavily in favour of the former, despite being used in equimolar amounts in **2**. All of the above suggests that examining increased ratios of base, the addition of oxidising agents (*e.g.* MnO_4^-), and the role of carboxylate sterics will be key in making new family members. The apparent preference of L^1 for M^{II} ions over M^{II} ions also suggests the ligand may be a good choice for targeting polymetallic Fe^{II} clusters.

Dc magnetic susceptibility and magnetisation measurements of polycrystalline samples of **1–3** reveal the predominance of antiferromagnetic exchange interactions. For **1** two very weak exchange interactions (J_1 = −0.19 cm^{-1}, J_2 = +0.038 cm^{-1}) lead to a diamagnetic S = 0 ground state with multiple low-lying excited states, assuming an isotropic model. A similar scenario, *i.e.* multiple weak magnetic interactions, is inferred for complex **2**, given the presence of numerous Mn^{II} ions. For **3** competing exchange interactions arising from the presence of multiple edge-sharing $[Mn_3]$ triangles, and the presence of multiple co-parallel JT axes, results in SMM behaviour with U_{eff} = 22 K (15.3 cm^{-1}).

Author contributions

EA performed the synthesis, GSN/ABC the single crystal XRD/PXRD measurements, respectively. EA/ABC collected and fitted the magnetic data. EKB conceived the idea. All authors contributed to the preparation of the manuscript.

Conflicts of interest

There are no conflicts to declare.

Acknowledgements

EKB thanks The Leverhulme Trust (RPG-2021-176).

Notes and references

1 (*a*) B. Bleaney and K. D. Bowers, *Proc. R. Soc. London, Ser. A*, 1952, **A214**, 451; (*b*) W. H. Crawford, H. W. Richardson, J. R. Wasson, D. J. Hodgson and W. E. Hatfield, *Inorg. Chem.*, 1976, **15**, 2107; (*c*) W. E. Hatfield, *Comments Inorg. Chem.*, 1981, **1**, 105; (*d*) J. Glerup, D. J. Hodgson and E. Petersen, *Acta Chem. Scand.*, 1983, **A37**, 161.
2 G. Aromí, S. M. J. Aubin, M. A. Bolcar, G. Christou, H. J. Eppley, K. Folting, D. N. Hendrickson, J. C. Huffman, R. C. Squire, H.-L. Tsai, S. Wang and M. W. Wemple, *Polyhedron*, 1998, **17**, 3005.
3 (*a*) A. Caneschi, D. Gatteschi, R. Sessoli, A.-L. Barra, L.-C. Brunel and M. J. Guillot, *J. Am. Chem. Soc.*, 1991, **113**, 5873; (*b*) R. Sessoli, H.-L. Tsai, A. R. Schake, S. Wang, J. B. Vincent, K. Folting, D. Gatteschi, G. Christou and D. N. Hendrickson, *J. Am. Chem. Soc.*, 1993, **115**, 1804; (*c*) R. Sessoli, D. Gatteschi, A. Caneschi and M. A. Novak, *Nature*, 1993, **365**, 141; (*d*) G. Christou, D. Gatteschi, D. N. Hendrickson and R. Sessoli, *MRS Bull.*, 2000, **25**, 66; (*e*) N. Ishikawa, M. Sugita, T. Ishikawa, S. Koshihara and Y. Kaizu, *J. Am. Chem. Soc.*, 2003, **125**, 8694; (*f*) J. M. Zadrozny and J. R. Long, *J. Am. Chem. Soc.*, 2011, **133**, 20732.
4 J. Schnack, *Dalton Trans.*, 2010, **39**, 4677.
5 M. Evangelisti and E. K. Brechin, *Dalton Trans.*, 2010, **39**, 4672.

6 (*a*) K. S. Pedersen, A.-M. Ariciu, S. McAdams, H. Weihe, J. Bendix, F. Tuna and S. Piligkos, *J. Am. Chem. Soc.*, 2016, **138**, 5801; (*b*) G. A. Timco, T. B. Faust, F. Tuna and R. E. P. Winpenny, *Chem. Soc. Rev.*, 2011, **40**, 3067.

7 (*a*) G. Aromí and E. K. Brechin, Synthesis of 3d Metallic Single-Molecule Magnets, in *Single-Molecule Magnets and Related Phenomena. Structure and Bonding*, ed. R. Winpenny, Springer, Berlin, Heidelberg, 2006, vol. 122; (*b*) C. J. Milios and R. E. P. Winpenny, Cluster-Based Single-Molecule Magnets, in *Molecular Nanomagnets and Related Phenomena. Structure and Bonding*, ed. S. Gao, Springer, Berlin, Heidelberg, 2014, vol. 164.

8 (*a*) N. Hoshino, A. M. Ako, A. K. Powell and H. Oshio, *Inorg. Chem.*, 2009, **48**, 3396; (*b*) C. Papatriantafyllopoulou, E. E. Moushi, G. Christou and A. J. Tasiopoulos, *Chem. Soc. Rev.*, 2016, **45**, 1597.

9 (*a*) R. Bagai and G. Christou, *Chem. Soc. Rev.*, 2009, **38**, 1011; (*b*) M. Affronte, F. Troiani, A. Ghirri, S. Carretta, P. Santini, V. Corradini, R. Schuecker, C. Muryn, G. Timco and R. E. Winpenny, *Dalton Trans.*, 2006, 2810–2817.

10 (*a*) A. J. Tasiopoulos and S. P. Perlepes, *Dalton Trans.*, 2008, 5537; (*b*) L. Ungur, S. K. Langley, T. N. Hooper, B. Moubaraki, E. K. Brechin, K. S. Murray and L. F. Chibotaru, *J. Am. Chem. Soc.*, 2012, **134**, 18554; (*c*) A. Baniodeh, N. Magnani, Y. Lan, G. Buth, C. E. Anson, J. Richter, M. Affronte, J. Schnack and A. K. Powell, *npj Quantum Mater.*, 2018, **3**, 10; (*d*) D. J. Cutler, M. K. Singh, G. S. Nichol, M. Evangelisti, J. Schnack, L. Cronin and E. K. Brechin, *Chem. Commun.*, 2021, **57**, 8925.

11 (*a*) E. K. Brechin, *Chem. Commun.*, 2005, 5141; (*b*) L. R. B. Wilson, M. Coletta, M. Evangelisiti, S. Piligkos, S. J. Dalgarno and E. K. Brechin, *Dalton Trans.*, 2022, **51**, 4213.

12 (*a*) C. J. Milios, T. C. Stamatatos and S. P. Perlepes, *Polyhedron*, 2006, **25**, 134; (*b*) R. Inglis, C. J. Milios, L. F. Jones, S. Piligkos and E. K. Brechin, *Chem. Commun.*, 2012, **48**, 181; (*c*) R. Inglis, S. M. Taylor, L. F. Jones, G. S. Papaefstathiou, S. P. Perlepes, S. Datta, S. Hill, W. Wernsdorfer and E. K. Brechin, *Dalton Trans.*, 2009, 9157.

13 (*a*) Y.-W. Li, L.-Y. Guo, L. Feng, Z. Jagličić, S.-Y. Zeng and D. Sun, *CrystEngComm*, 2017, **19**, 5897; (*b*) W.-F. Xie, L.-Y. Guo, J.-H. Xu, M. Jagodič, Z. Jagličić, W.-G. Wang, G.-L. Zhuang, Z. Wang, C.-H. Tung and D. Sun, *Eur. J. Inorg. Chem.*, 2016, 3253; (*c*) B. Barszcz, T. Głowiak, J. Jezierska and A. Tomkiewicz, *Polyhedron*, 2004, **23**, 1309; (*d*) I. Banerjee, M. Dolai, A. D. Jana, K. K. Das and M. Ali, *CrystEngComm*, 2012, **14**, 4972; (*e*) B. Barszcz, T. Głowiak, J. Jezierska and K. Kurdziel, *Inorg. Chem. Commun.*, 2002, 1056–1058; (*f*) V. M. Leovac, R. Petković, A. Kovács, G. Pokol and K. M. Szécsény, *J. Therm. Anal. Calorim.*, 2007, **89**, 267; (*g*) R. W. M. ten Hoedt, F. B. Hulsbergen, G. C. Verschoor and J. Reedijk, *Inorg. Chem.*, 1982, **21**, 2369; (*h*) A. Beheshti, E. S. M. Fard, M. Kubicki, P. Mayer, C. T. Abrahams and S. E. Razatofighie, *CrystEngComm*, 2019, **21**, 251; (*i*) J. Lim, G. Kim, K. Do, S. Lee, S. Ryu, D. Yoshioka and M. Mikuriya, *X-Ray Struct. Anal. Online*, 2015, **31**, 49; (*j*) A. Mar, S. J. Retting, A. Storr and J. Trott, *Can. J. Chem.*, 1988, **66**, 101; (*k*) F. Paap, E. Bouwman, W. L. Driessen, R. A. G. de Graaff and J. Reedijk, *J. Chem. Soc., Dalton Trans.*, 1985, 737.

14 R. Touzani, M. Haibach, A. J. Nawara-Hultzsch, S. El Kadiri, T. J. Emge and A. S. Goldman, *Polyhedron*, 2011, **30**, 2530.

15 (*a*) L.-Y. Guo, H.-F. Su, M. Kurmoo, C.-H. Tung, D. Sun and L.-S. Zheng, *J. Am. Chem. Soc.*, 2017, **139**, 14033–14036; (*b*) F. Yang, Y.-K. Deng, L.-Y. Guo, H.-F. Su, Z. Jagličić, Z.-Y. Feng, G.-L. Zhuang, S.-Y. Zenge and D. Sun, *CrystEngComm*, 2016, **18**, 1329; (*c*) B.-Q. Ji, H.-F. Su, M. Jagodič, Z. Jaglicič, M. Kurmoo, X.-P. Wang, C.-H. Tung, Z.-Z. Cao and D. Sun, *Inorg. Chem.*, 2019, **58**, 3800; (*d*) Y.-K. Deng, H.-F. Su, J.-H. Xu, W.-G. Wang, M. Kurmoo, S.-C. Lin, Y.-Z. Tan, J. Jia, D. Sun and L.-S. Zheng, *J. Am. Chem. Soc.*, 2016, **138**, 1328.

16 W. L. Driessen, *Recl. Trav. Chim. Pays-Bas*, 1982, **101**, 441.

17 (*a*) G. M. Sheldrick, *Acta Crystallogr., Sect. A: Found. Adv.*, 2015, **A71**, 3; (*b*) O. V. Dolomanov, L. J. Bourhis, R. J. Gildea, J. A. K. Howard and H. Puschmann, *J. Appl. Crystallogr.*, 2009, **42**, 339; (*c*) G. M. Sheldrick, *Acta Crystallogr., Sect. C: Struct. Chem.*, 2015, **C71**, 3.

18 (*a*) A. R. E. Baikie, A. J. Howes, M. B. Hursthouse, A. B. Quick and P. Thornton, *J. Chem. Soc., Chem. Commun.*, 1986, 1587; (*b*) A. G. Blackman, J. C. Huffman, E. B. Lobkovsky and G. Christou, *Polyhedron*, 1992, **11**, 251.

19 (*a*) S.-H. Huang, C.-I. Yang, S.-Y. Jhan and H.-L. Tsai, *Polyhedron*, 2013, **66**, 245; (*b*) M. Charalambous, E. E. Moushi, T. N. Nguyen, A. M. Mowson, G. Christou and A. J. Tasiopoulos, *Eur. J. Inorg. Chem.*, 2018, 3905; (*c*) M. Manoli, A. Collins, S. Parsons, A. Candini, M. Evangelisti and E. K. Brechin, *J. Am. Chem. Soc.*, 2088, **130**, 11129; (*d*) Y. Okui, F. A. Catusanu, R. Kubota, B. Kure, T. Nakajima, T. Tanase, T. Kajiwara, M. Mikuriya, H. Miyasaka and M. Yamashita, *Eur. J. Inorg. Chem.*, 2011, 4325; (*e*) L. Zhang, R. Clérac, P. Heijboer and W. Schmitt, *Angew. Chem., Int. Ed.*, 2012, **51**, 3007; (*f*) A. Mishra, J. Yano, Y. Pushkar, V. K. Yachandra, K. A. Abboud and G. Christou, *Chem. Commun.*, 2007, 1538; (*g*) A. Mishra, Y. Pushkar, J. Yano, V. K. Yachandra, W. Wernsdorfer, K. A. Abboud and G. Christou, *Inorg. Chem.*, 2008, **47**, 1940; (*h*) K. Su, F. Jiang, J. Qian, J. Pan, J. Pang, X. Wan, F. Hu and M. Hong, *RSC Adv.*, 2015, **5**, 33579; (*i*) C. C. Stoumpos, I. A. Gass, C. J. Milios, N. Lalioti, A. Terzis, G. Aromi, S. J. Teat, E. K. Brechin and S. P. Perlepes, *Dalton Trans.*, 2009, 307; (*j*) C. J. Milios, E. Kefalloniti, C. P. Raptopoulou, A. Terzis, R. Vicente, N. Lalioti, A. Escuer and S. P. Perlepes, *Chem. Commun.*, 2003, 819; (*k*) D. I. Alexandropoulos, C. Papatriantafyllopoulou, C. Li, L. Cunha-Silva, M. J. Manos, A. J. Tasiopoulos, W. Wernsdorfer, G. Christou and T. C. Stamatatos, *Eur. J. Inorg. Chem.*, 2013, 2286; (*l*) M. U. Anwar, Y. Lan, L. M. C. Beltran, R. Clérac, S. Pfirrmann, C. E. Anson and A. K. Powell, *Inorg. Chem.*, 2009, **48**, 5177; (*m*) F.-P. Xiao and L.-F. Jin, *Inorg. Chem. Commun.*, 2008, **11**, 717;

(*n*) X. Jiang, G.-Y. An, C.-M. Liu and H.-Z. Kou, *Eur. J. Inorg. Chem.*, 2015, 5314; (*o*) J. S. Costa, L. A. Barrios, G. A. Craig, S. J. Teat, F. Luis, O. Roubeau, M. Evangelisti, A. Camon and G. Aromí, *Chem. Commun.*, 2012, **48**, 1413; (*p*) G. Aromí, A. Bell, S. J. Teat, A. G. Whittaker and R. E. P. Winpenny, *Chem. Commun.*, 2002, 1896; (*q*) X.-Y. Wang, A. V. Prosvirin and K. R. Dunbar, *Angew. Chem., Int. Ed.*, 2010, **49**, 5081.

20 (*a*) S. K. Langley, K. J. Berry, B. Moubaraki and K. S. Murray, *Dalton Trans.*, 2009, 973; (*b*) T. Stamatatos, D. Foguet-Albiol, W. Wernsdorfer, K. A. Abboud and G. Christou, *Chem. Commun.*, 2011, **47**, 274.

21 M. Manoli, R. Inglis, S. Piligkos, L. Yanhua, W. Wernsdorfer, E. K. Brechin and A. J. Tasiopoulos, *Chem. Commun.*, 2016, **52**, 12829.

22 C.-M. Liu, D.-Q. Zhang and D.-B. Zhu, *Chem. – Asian J.*, 2011, **6**, 74.

23 M. Shanmugam, G. Chastanet, T. Mallah, R. Sessoli, S. J. Teat, G. A. Timco and R. E. P. Winpenny, *Chem. – Eur. J.*, 2006, **12**, 8777.

24 (*a*) H. J. Eppley, N. de Vries, S. Wang, S. M. Aubin, H.-L. Tsai, K. Folting, D. N. Hendrickson and G. Christou, *Inorg. Chim. Acta*, 1997, **263**, 323; (*b*) A. M. Ako, B. Burger, Y. Lan, V. Mereacre, R. Clérac, G. Buth, S. Gomez-Coca, E. Ruiz, C. E. Anson and A. K. Powell, *Inorg. Chem.*, 2013, **52**, 5764.

25 E. K. Brechin, W. Clegg, M. Murrie, S. Parsons, S. J. Teat and R. E. P. Winpenny, *J. Am. Chem. Soc.*, 1998, **120**, 7365.

26 A.-J. Zhou, J.-D. Leng, J.-S. Hu and M.-L. Tong, *Dalton Trans.*, 2013, **42**, 9428.

27 R. C. Squire, S. M. J. Aubin, K. Folting, W. E. Streib, D. N. Hendrickson and G. Christou, *Angew. Chem., Int. Ed. Engl.*, 1995, **34**, 887.

28 (*a*) E. K. Brechin, C. Boskovic, W. Wernsdorfer, J. Yoo, A. Yamaguchi, E. C. Sañudo, T. R. Concolino, A. L. Rheingold, H. Ishimoto, D. N. Hendrickson and G. Christou, *J. Am. Chem. Soc.*, 2002, **124**, 9710; (*b*) E. K. Brechin, E. C. Sañudo, W. Wernsdorfer, C. Boskovic, J. Yoo, D. N. Hendrickson, A. Yamaguchi, H. Ishimoto, T. E. Concolino, A. L. Rheingold and G. Christou, *Inorg. Chem.*, 2005, **44**, 502; (*c*) E. C. Sanudo, E. K. Brechin, C. Boskovic, W. Wernsdorfer, J. Yoo, A. Yamaguchi, T. R. Concolino, K. A. Abboud, A. L. Rheingold, H. Ishimoto, D. N. Hendrickson and G. Christou, *Polyhedron*, 2003, **22**, 2267.

29 (*a*) M. Nihei, N. Hoshino, T. Ito and H. Oshio, *Polyhedron*, 2003, **22**, 2359; (*b*) G. S. Papaefstathiou, A. Escuer, F. A. Mautner, C. Raptopoulou, A. Terzis, S. P. Perlepes and R. Vicente, *Eur. J. Inorg. Chem.*, 2005, 879; (*c*) D. Sivanesan, K. Son, H. J. Lee, K. T. Park, Z. Jang, B. J. Suh and S. Yoon, *Polyhedron*, 2013, **50**, 339; (*d*) C. C. Stoumpos, I. A. Gass, C. J. Milios, N. Lalioti, A. Terzis, G. Aromí, S. J. Teat, E. K. Brechin and S. P. Perlepes, *Dalton Trans.*, 2009, **2**, 307; (*e*) T. Taguchi, M. R. Daniels, K. A. Abboud and G. Christou, *Inorg. Chem.*, 2009, **48**, 9325.

30 (*a*) A. Abragam and B. Bleaney, *Electron Paramagnetic Resonance of Transition Ions*, Clarendon Press, Oxford, 1970; (*b*) F. E. Mabbs and D. Collison, *Electron Paramagnetic Resonance of d Transition Metal Compounds*, Elsevier, Amsterdam, 1992; (*c*) C. Duboc, M.-N. Collomb and F. Neese, *Appl. Magn. Reson.*, 2010, **37**, 229; (*d*) R. Boča, *Coord. Chem. Rev.*, 2004, **248**, 757.

31 (*a*) M. Soler, E. Rumberger, K. Folting, D. N. Hendrickson and G. Christou, *Polyhedron*, 2001, **20**, 1365; (*b*) C. Boskovic, E. K. Brechin, W. E. Streib, K. Folting, J. C. Bollinger, D. N. Hendrickson and G. Christou, *J. Am. Chem. Soc.*, 2002, **124**, 3725.

32 D. Reta and N. F. Chilton, *Phys. Chem. Chem. Phys.*, 2019, **21**, 23567–23575.

33 See for example: (*a*) S. M. Taylor, R. D. McIntosh, S. Piligkos, S. J. Dalgarno and E. K. Brechin, *Chem. Commun.*, 2012, **48**, 11190; (*b*) C. Boskovic, E. K. Brechin, W. E. Streib, K. Folting, D. N. Hendrickson and G. Christou, *Chem. Commun.*, 2001, 467–468; (*c*) E. K. Brechin, J. C. Huffman, G. Christou, J. Yoo, M. Nakano and D. N. Hendrickson, *Chem. Commun.*, 1999, 783; (*d*) C. Boskovic, E. K. Brechin, W. E. Streib, K. Folting, J. C. Bollinger, D. N. Hendrickson and G. Christou, *J. Am. Chem. Soc.*, 2002, **124**, 3725; (*e*) J. Yoo, E. K. Brechin, A. Yamaguchi, M. Nakano, J. C. Huffman, A. L. Maniero, L.-C. Brunel, K. Awaga, H. Ishimoto, G. Christou and D. N. Hendrickson, *Inorg. Chem.*, 2000, **39**, 3615–3623.